Fermilab Library
0 1160 0072930 5

TRI-PP-95-2
Jan 1995

Magnetic trapping of spin-polarized neutral atoms and its limits

V. E. Shapiro

TRIUMF, 4004 Wesbrook Mall, Vancouver, B.C., Canada V6T 2A3

FERMILAB
MAR 1
LIBRA

Abstract

We investigated the limits of magnetic methods of trapping neutral atoms in a spot of small size and small polarization misalignment. The analysis covers various methods of trapping with static and rotating magnetic field. In particular, new rotating field methods having advantages are proposed. They differ from the recently invented "top" type by employing a slow rotating field, resonant to the orbiting atoms, rather than much faster rotation. Also a theory of the top trap is developed. It elucidates important features of trapping lying beyond the time-averaged potential concept. General criteria on the trapping temperature as a function of size and misalignment parameters are established for various methods.

(Submitted to Physical Review A)

PACS numbers: 32.80.Pj, 85.70.Nk, 42.50.Vk

TRI-PP-95-2

I. INTRODUCTION

The method of neutral atom trapping by magnetic fields has been successfully demonstrated since 1985 [1-3] and its usage and development is in rapid progress, (see e.g. Refs. [4-7]). Many questions have arisen and there are many factors to consider if requirements on the smallness of atom spot and polarization misalignment are imposed. First of all, the question about the most appropriate magnetic field configuration is very important since the magnetic potential well is shallow and able to trap only atoms of rather low temperatures $\sim 10^{-3}$ K. Even deeper cooling of the atoms is required if low polarization misalignment is critical.

Addressing the problem, we derive simple criteria and present scales and estimates allowing one to judge and compare various types of magnetostatic traps. We consider the static field traps and the type with rotating field ("top" trap) recently invented by Cornell [7] and investigated very sketchily in the literature. The top trap is considered in more detail and its new features are elucidated. We also draw attention to trapping methods with rotating fields of much lower frequency than the top type. These methods are discussed for the first time. Our earlier results reported to the TRIUMF TRINAT group and summarized in [8] are partly included in the present consideration.

II. MAIN ASSUMPTIONS AND DEFINITIONS

The well-known principle behind a magnetic trap is that magnetic dipoles may be trapped by a local field minimum (local maxima are forbidden) and that the atoms prepared in select Zeeman levels with the resultant (average) magnetic moment $\boldsymbol{\mu}$ antiparallel to an applied magnetic field $\boldsymbol{B}$ follow adiabatically the magnetic field lines across the volume of the trap. In such states the atoms are attracted to a point of minimum of the force potential

$$U(\boldsymbol{r}) = -\boldsymbol{\mu}\boldsymbol{B}(\boldsymbol{r}) + Mgz = \mu B(\boldsymbol{r}) + Mgz \tag{1}$$

with $B = |\boldsymbol{B}|$ and $\mu = |\boldsymbol{\mu}| = \text{const} > 0$, i.e. to a minimum of the magnetic field magnitude (here M is the atomic mass, g the gravity acceleration). The model can be applied to the case of slow time-varying fields, in which the frequency spectrum of $\boldsymbol{B}(t) = \boldsymbol{B}(\boldsymbol{r}(t), t)$ for a trapped atom is in a range well below the Zeeman frequency in the field. This is what one means by a magnetostatic trap. The trapped atoms are vulnerable to background gas collisions and the mean free time between collisions should exceed the desired trapping time.

We will first consider static field traps. At the trap centre

$$\frac{\partial B}{\partial z} = -\frac{Mg}{\mu}. \tag{2}$$

Also, the curvature of the field B at the trap centre should be positive to provide confinement in three orthogonal directions. The curvature is given by the matrix $\partial^2 B/\partial r_i \partial r_k$. In the coordinate frame where the matrix is diagonal the natural frequencies of small amplitude atomic oscillation are given by

$$\omega_i = \sqrt{\frac{\mu}{M}\frac{\partial^2 B}{\partial r_i^2}}. \tag{3}$$

We will assume that the directions r_i coincide with the coordinate frame x, y, z and the point $\boldsymbol{r} = 0$ will be taken at the trap centre.

The lower edge of the potential well of $U(\boldsymbol{r})$ Eq. (1) is located where Eq. (2) is again satisfied, after the field curvature changes sign. The upper edge may be at infinity, or where the field goes through a maximum, again satisfying equation (2). One more edge leading to the leakage of particles is in the vicinity of $B = 0$ where the adiabaticity is violated. What one usually needs is for the well to be as deep as possible within a given atom spot size, rather than a deep well with a wider but flat bottom. Requirements on the uniformity of atom polarization alignment within the atom spot reinforce this point. In particular, the "hole" centered at $B = 0$ should not be inside the atom spot, and neither should the field curvature vary considerably inside.

In the case of a small atom spot, its average spatial scales $\overline{r_i^2}$ are related to the trapping temperatures T_i by

$$kT_i = M\overline{\dot{r}_i^2(0)} = 2M\omega_i^2\overline{r_i^2}\,. \tag{4}$$

We define the trapping temperature such that $kT_i/2$ is the total initial kinetic energy of the atoms, divided by the number of atoms loaded into the trap centre. The conditions correspond to the loading from an optical trap having much better confinement. The energy of oscillation is distributed equally, in average, between the kinetic and potential energy and this results in the factor 2 in Eq. (4). The definition does not depend on interactions between atoms and whether thermalization takes place. Obviously, the requirements on preliminary cooling of the trapped atoms are directly related to the trapping temperatures, specifically their upper bounds for given spot sizes and polarization misalignment. Our goal will be to determine such bounds.

The accuracy of Eq. (4) can be judged by the frequency shift $\delta\omega_i/\omega_i$ caused by anharmonicity. For small $\overline{r^2}$, $|\delta\omega_i|/\omega_i = \overline{r^2}/l^2$, roughly, where l is a characteristic scale of field curvature variation. For typical trapping geometries l is about three times smaller than R, the radius of the "main" magnetic coil, so for amplitudes, $\sqrt{\overline{r^2}}$, not larger than $\sim 0.1R$ we may rely on Eq. (4). In fact the atom spot sizes of interest are within this scale.

The static field traps of interest employ the field $\boldsymbol{B}(0)$ aligned vertically, and as a measure of deviation of atomic polarization from z-alignment within the spot, we will take the quantity

$$P = 1 - \left|\overline{\mu_z(\boldsymbol{r})}\right| \Big/ \mu = 1 - \left|\overline{B_z(\boldsymbol{r})/B(\boldsymbol{r})}\right|$$

which in the case of small atom spots reduces to

$$P = \frac{1}{2}\left|\sum_{r_i=x,y,z} \overline{r_i^2}\,\frac{\partial^2}{\partial r_i^2}\frac{B_z}{B}\right| \tag{5}$$

where the derivatives are taken at $\boldsymbol{r} = 0$.

Proceeding from these notions and definitions we will consider first, in Secs. II-V, the static field traps. The rotating field traps require a modified approach which is undertaken in Secs. VI and VII.

III. THE AXIAL SYMMETRY TRAP

The magnetic coil configuration we address here is a set of concentric coils of arbitrary radii and currents with the axis in the z direction. Simple examples are the "opposing coils"

and "spherical hexapole" traps (Fig. 1(a,b)). Obviously, the arrangements with $B(0) = 0$, e.g. the spherical quadrupole of such currents that $\partial B/\partial z$ at the quadrupole centre satisfies Eq. (2), do not do for the traps of interest. The analysis below makes this and other requirements clear and puts them on a quantitative basis. The quadrupole configuration is merely one of the axial symmetry traps. Coils with parallel currents, rather than opposing, is an example of different trap configuration.

The magnetic field components near the axis can be presented up to second order in $r_\perp$ by the well-known general expansion

$$B_z(z, r_\perp) = B_o(z) - \frac{1}{4}B_o''(z)r_\perp^2,$$

$$B_x(z, r_\perp) = -\frac{1}{2}B_o'(z)x, \quad B_y(z, r_\perp) = -\frac{1}{2}B_o'(z)y$$

where $r_\perp^2 = x^2 + y^2$, $B_o(z)$ is the magnetic field at the axis of symmetry, $B_o'(z) = dB_o(z)/dz$ and $B_o''(z) = d^2B_o(z)/dz^2$. These quantities at the trap centre are related through Eqs. (2) and (3), yielding

$$\frac{B_oB_o'}{|B_o|} = -\frac{Mg}{\mu},$$

$$\omega_z^2 = \frac{\mu}{M}\frac{B_o''B_o}{|B_o|},$$

$$\omega_x^2 = \omega_y^2 = \frac{\mu}{M}\frac{B_o'^2 - 2B_o''B_o}{4|B_o|}.$$

As a consequence,

$$B_o'^2 > 2B_oB_o'' > 0, \quad B_o'^2 = (Mg/\mu)^2. \tag{6}$$

Evaluating P of Eq. (5) and relating $\overline{r_\perp^2}$ to the perpendicular temperature $T_\perp = (T_x + T_y)/2$ via definition (4) one obtains

$$P = \frac{B_o'^2}{8B_o^2}\overline{r_\perp^2} = \frac{kT_\perp}{2\mu|B_o|}\left(1 + \frac{\omega_z^2}{2\omega_x^2}\right).$$

Excluding B_o (using the latter relation), results in

$$\frac{kT_\perp}{Mg\sqrt{\overline{r_\perp^2}/2}} = c_1\sqrt{P}, \quad \text{where} \quad c_1 = \frac{\omega_x^2}{\omega_x^2 + \omega_z^2/2}. \tag{7}$$

This relation allows one to determine the trapping temperature required to provide a given (small) atom spot size and misalignment. Its upper bound is given by

$$T_\perp = \frac{Mg}{k}\sqrt{P\overline{r_\perp^2}/2} \sim 0.4 \times 10^{-4}\ \text{K}. \tag{8}$$

llere (and further on) the numerical estimates are for $M = 40$ a.m.u. We assume in Eq. (8) that $\sqrt{\overline{r_\perp^2}} = 0.5$ cm and $P = 0.05$.

We may also interpret the relations (7) and (8) as a bound on the product $P\overline{r_\perp^2}$ for a given trapping temperature $T_\perp$:

$$\sqrt{P\overline{r_\perp^2}/2} = \frac{kT_\perp}{Mgc_1} < \frac{kT_\perp}{Mg}. \tag{9}$$

Similarly, the product $P\overline{z^2}$ can be presented in the form

$$\sqrt{P\overline{z^2}} = \frac{k\sqrt{T_z T_\perp}}{Mg}\frac{\omega_x^2 + \omega_z^2/2}{\omega_x\omega_z} < \frac{k\sqrt{2T_z T_\perp}}{Mg} \tag{10}$$

where, however, $T_\perp$ is bounded by Eqs. (7) and (8).

No dependence on the magnetic field appears and only one atomic parameter, the atomic mass, enters Eq. (8) as well as the r.h.s. of Eqs. (9) and (10). Originally we came to this result by a different approach [8]. Thus, whatever the set of concentric coils, their radii and currents are, the relation (7) and its consequence Eqs. (8), (9) and (10) is true. With this the derivation implies that the magnetic field provides trapping and the atom spot is small compared with the spatial scales of oscillation anharmonicity of atoms in the trap.

The formulas (7)-(10) seem in evident contradiction with the case $g = 0$. But in that case $B_o' = 0$ and the requirement (6) cannot be satisfied, i.e. a trap of axial symmetry with the desired properties cannot be realized.

The larger the atomic mass M, the higher the temperature that can be used for trapping. In principle, the derivation is applicable to a macroscopic particle, provided its state with $\boldsymbol{\mu}$ antiparallel to $\boldsymbol{B}$ and $\mu = \text{const}$ has a sufficient life-time. Note that the bound Eq. (8) written in terms of mean square velocity rather than temperature is a universal function entirely independent of free parameters:

$$\overline{v^2} = 3g\sqrt{P\overline{r_\perp^2}/2}$$

which for $P = 0.05$ and $\sqrt{\overline{r_\perp^2}} = 0.5$ cm results in $\sqrt{\overline{v^2}} \approx 15$ cm/sec.

IV. THE "COIL + CURRENT BAR" TRAP

The magnetic field coil configuration considered here has vertical current bars which generate a quadrupole field in the horizontal plane (Fig. 2(a)). The vertical field is formed mainly by the current of a round coil so that to second order in coordinates

$$\begin{aligned} B_z &= B_o(z) - \frac{1}{4}B_o''(z)r_\perp^2, \\ B_x &= -\left(\frac{1}{2}B_o'(z) + Q\right)x, \\ B_y &= -\left(\frac{1}{2}B_o'(z) - Q\right)y \end{aligned} \tag{11}$$

where $(Qx, -Qy)$ are the components of the quadrupole field and $B_o(z)$ is the axial field of the round coil. For a thin coil of radius R placed at $z = -D$

$$B_o(z) = \left(\frac{D^2 + R^2}{(D+z)^2 + R^2}\right)^{3/2} B_o$$

with $B_o = B(0)$ determined via the condition Eq. (2). As a result

$$\omega_z^2 = \frac{g}{L}, \quad \text{where} \quad L = D\frac{D^2 + R^2}{4D^2 - R^2} \tag{12}$$

and in view of Eq. (4) we obtain the relation

$$\frac{kT_z}{Mg\sqrt{\overline{z^2}}} = \frac{2\sqrt{\overline{z^2}}}{L}. \tag{13}$$

Obviously, the area of interest and applicability of Eq. (13) is where $\sqrt{\overline{z^2}}$ is small compared with L. One may use Eq. (13) where Eq. (4) can be used (i.e. where $\sqrt{\overline{z^2}} \sim 0.1D$ or smaller). The spatial scale L is bounded by the fact that $D > R/2$ and that the coil radius R cannot in practice be made arbitrarily small. For a given R the minimum of L is $\approx R/3$, for $D^2/R^2 = 2/(\sqrt{65} - 7) \approx 2$. Thus, the relation (13) imposes by itself, without any additional restriction on polarization misalignment, a strong bound on the trapping temperature. For $R = D = 5$ cm and the spot size $\sqrt{\overline{z^2}} = 0.5$ cm the bound equals

$$T_z = \frac{Mg}{k}\frac{3\overline{z^2}}{D} \sim 0.7 \times 10^{-4}\ K.$$

Requirements for small polarization misalignment impose upper bounds on the trapping temperatures T_x, T_y rather than T_z. Evaluating p of Eq. (5) for an atom spot of temperature $T_x = T_y = T_\perp$ we obtain

$$P = \frac{kT_\perp}{2\mu|B_o|}c_2, \quad \text{where} \quad c_2 = 1 + \frac{\omega_z^2}{4\omega_x^2} + \frac{\omega_z^2}{4\omega_y^2}.$$

With B_o determined via Eq. (2) this results in the following bound

$$T_\perp = \frac{Mg}{k}\frac{2L_1}{c_2}P \sim 0.8 \times 10^{-4}\ K \tag{14}$$

where

$$L_1 = L\frac{4D^2 - R^2}{3D^2}$$

and the numerical example is for $R = D = 5$ cm, $c_2 = 2$ and $P = 0.05$. It is worth noting that the product $P\overline{z^2}$ is given by the formula similar to (10)

$$\sqrt{P\overline{z^2}} = \frac{k\sqrt{T_z T_\perp}}{Mg}\sqrt{\frac{c_2}{4}\frac{3D^2}{4D^2 - R^2}}$$

where T_z and $T_\perp$ are bounded by Eqs. (13) and (14).

Again, as for the axial symmetry traps, the upper bounds on the trapping temperatures do not depend on the magnetic field magnitude, and only one atomic parameter, the mass M, enters the criteria for T_z and $T_\perp$.

V. THE "BASEBALL", AND OTHER STATIC FIELD TRAPS

The "baseball" geometry consists of a loop of wire wound similar to the seams of a baseball (Fig. 2(b)) and an axial pair of anti-Helmholtz coils to generate the required axial field to compensate gravity at the baseball centre. The baseball loop current produces no field gradient at the centre, just field and field curvature, and so this point is the centre of the trap. The anti-Helmholtz coils generate no field or curvature, and thus the curvature is decoupled from the gradient, unlike previously discussed configurations.

The field expansion near the trap centre is given, to second order in coordinates, by the functional form Eq. (11), whereas before $|B_o'| = Mg/\mu$, while B_o, B_o'' and Q are determined by the baseball coil radius R and current I by

$$B_o = \frac{2I}{5R}, \quad B_o'' = \frac{2B_o}{R^2}, \quad Q = \frac{5B_o}{2R}. \tag{15}$$

The natural frequencies ω_i (Eq. (3)) take the form

$$\omega_z^2 = \frac{\mu}{M} B_o'', \quad \omega_\pm^2 = \frac{\mu}{M} \frac{(Q \pm \frac{Mg}{2\mu})^2}{B_o} - \frac{\omega_z^2}{2} \tag{16}$$

where $\omega_\pm = \omega_{x,y}$ and B_o and B_o'' are assumed (without loss of generality) positive. At $B_o \leq 2MgR/3R$ the dimension y becomes untrapped. In the limit of large B_o and, hence, large Q, the frequencies $\omega_\pm$ become equal and three times larger than ω_z.

From (4), (15) and (16) follows the relation

$$T_z = \frac{2\mu B_o}{k} \frac{\overline{z^2}}{R^2} \sim 2.7 \times 10^{-4} K. \tag{17}$$

The numerical estimate is for $R = 5$ cm, $\sqrt{\overline{z^2}} = 0.5$ cm, $\mu = \mu_B$, the Bohr magneton, and $B_o = 10^2$ gauss. Such a baseball field is generated by the current $I = 5B_oR/2 = 1250$ ampere-turns. To increase it by much creates technical problems, so the cited figure of T_z seems a characteristic scale for the baseball traps.

Now let us investigate the polarization characteristic of Eq. (5). For the baseball trap we obtain

$$P = \frac{k}{4\mu B_o} \left[T_x \left(1 + \frac{\omega_z^2}{2\omega_+^2}\right) + T_y \left(1 + \frac{\omega_z^2}{2\omega_-^2}\right) \right]. \tag{18}$$

It follows that the upper temperature bound is given by

$$T_\perp = \frac{2\mu B_o}{k} P \sim 7 \times 10^{-4} \text{ K}$$

where the numerical example is the same as in Eq. (17) with $P = 0.05$. Since the cited horizontal temperature bound is 2.5 times larger than the corresponding vertical temperature bound in (17), the level of polarization misalignment, for the given vertical size spot and isotropic trapping temperature, is much better than for $P = 0.05$.

Finally, we note that the baseball trap and the traps employing a bias field B_o and axial confinement from a set of concentric coils and transverse confinement from a four-wire quadrupole field have much in common, in particular the relations (11), (16) and (18) are the same. An example is the Ioffe trap, which has two concentric coils with equal currents (Fig. 2(c)). As seen from Eqs. (16) and (18) the bias field should be within certain limits to provide both small spot size and polarization misalignment and therefore, though more freedom in the parameters of B_o and ω_i appear, the upper temperature bounds cannot change much compared with the case of the baseball trap.

VI. THE TOP TRAP

The top ("time-averaged orbiting potential") trap is a recent invention [7]. It employs a combination of static and rotating magnetic fields:

$$\boldsymbol{B}(\boldsymbol{r}, t) = \boldsymbol{B}_{oc}(\boldsymbol{r}) + \boldsymbol{b}(t) \tag{19}$$

where $\boldsymbol{B}_{oc}$ is an axial quadrupole field generated by "opposing coils" with the axis in the vertical direction (Fig. 1(a)) and $\boldsymbol{b}$ is a large-amplitude uniform field quickly rotating in the horizontal plane. "Large" and "quickly" are in the sense

$$b^2 \gg B_o^2, \quad \omega_i \ll \Omega \ll \Omega_Z \tag{20}$$

where $B_o = B_{oc}(0)$ is the vertical field at the trap centre, Ω is the frequency of rotation of the field $\boldsymbol{b}$, Ω_Z the Zeeman splitting in the field and ω_i with $i = x, y, z$ are the natural frequencies of small amplitude smoothed vibration. The inequality $\Omega \ll \Omega_Z$ makes the principle behind the top trap the same as for a static field trap. The atomic magnetic moment adiabatically follows the field rotation which in view of $b^2 \gg B_o^2$ rotates almost in the horizontal plane. The top trap has a rather small atom spot. This and the rotation of the atomic polarization are attractive features for experiments on polarized neutral atoms.

Now, unlike the static field traps, the potential $U(\boldsymbol{r})$ Eq. (1) varies periodically in time. That the oscillating component of magnetic force is large and influences the confinement critically makes the analysis of confinement more complex than that of a static field trap. The atom motion $\boldsymbol{r}(t)$ is a superposition of a high frequency, small radius orbit and a smoothed oscillation in the averaged potential characterized by low frequencies $\omega_i \ll \Omega$. The standard asymptotic method of nonlinear mechanics can be applied to the analysis and we used it at first. However, the conventional second order perturbation theory results in losing sight of interesting features elucidated below. We obtained them by a different method - employing the coordinate frame rotating with the field. This greatly simplifies the analysis and its correctness becomes easy to check, because the confinement is then governed by the time-independent potential

$$U(\boldsymbol{R}) = \mu B(\boldsymbol{R}) - \frac{1}{2} M\Omega^2 (X^2 + Y^2) + Mgz \tag{21}$$

with $B(\boldsymbol{R}) = B(\boldsymbol{r}, t)$, $\boldsymbol{R} = (X, Y, z)$ and the second term in the r.h.s. representing the centrifugal forces. Assuming the static field configuration an axial quadrupole, the total field $\boldsymbol{B}(\boldsymbol{R})$ components read

$$B_X = b - \frac{1}{2} B_o' X, \quad B_Y = -\frac{1}{2} B_o' Y, \quad B_z = B_o + B_o' z. \tag{22}$$

The coordinates X, Y are expressed via x, y by

$$(X, Y) = \Big(x\cos(\Omega t) + y\sin(\Omega t),\ -x\sin(\Omega t) + y\cos(\Omega t) \Big),$$

if $t = 0$ is taken as a moment where $\boldsymbol{b}$ is directed along x.

Neglecting other influences, the atomic motion equation takes the form

$$\ddot{\boldsymbol{R}} = -\frac{1}{M} \frac{\partial U}{\partial \boldsymbol{R}} - 2[\boldsymbol{\Omega} \times \dot{\boldsymbol{R}}]. \tag{23}$$

The second term in the r.h.s. is the Coriolis force and $\boldsymbol{\Omega} = (0, 0, \Omega)$. The equilibrium point $\boldsymbol{R} = \boldsymbol{R}_o$ of Eq. (23), determined by $\partial U/\partial \boldsymbol{R} = 0$, corresponds to the synchronous rotation of trapped atoms about axis z at frequency Ω. Taking $\boldsymbol{R} = 0$ for the center of rotation, we obtain $\boldsymbol{R}_o = (X_o, 0, 0)$ where X_o is determined from

$$X_o = -\frac{2b}{B_o'}\frac{2\omega_o^2(X_o)}{\Omega^2 - 2\omega_o^2(X_o)} \tag{24}$$

with

$$\omega_o^2 = \frac{\mu}{8M}\frac{B_o'^2}{\overline{B}} \quad \text{and} \quad \overline{B} = B(\boldsymbol{R}_o).$$

The frequency ω_o characterizes the transverse oscillation $\boldsymbol{r}(t)$ in the potential $U(\boldsymbol{r}, t)$ averaged over explicit t dependence. The regime of fast rotation implies $\omega_o \ll \Omega$ and hence $B_o' X_o \ll b$. Because of that and in view of $B_o \ll b$ it follows $B(\boldsymbol{R}_o) \approx b$ and $\omega_o(X_o) \approx \omega_o(0)$.

The equation $\partial U(\boldsymbol{R})/\partial z = 0$ takes the form

$$B_o' = -\frac{Mg}{\mu}\frac{\overline{B}}{B_o} \tag{25}$$

and represents the balance condition between the gravitational and magnetic forces. It differs from that of the static field traps, Eq. (2), considerably since $\overline{B} \gg B_o$ and it is no harm for the top trap to have B_o arbitrary small. While for the static traps B_o' is fixed by atomic parameters, the B_o' of Eq. (25) is not. This equation may be viewed as a relation between B_o', b and B_o. The larger B_o' is, the larger the confinement spring ω_o^2 which behaves like $B_o'^2/\overline{B} \approx (Mg/\mu)^2 b/B_o$.

Let us consider small oscillation near the state $\boldsymbol{R} = \boldsymbol{R}_o$. Linearizing Eq. (23) we arrive at the system of three coupled oscillators

$$\begin{aligned} \ddot{X} + (2\Delta^2 - \Omega^2)(X - X_o) &= 2\Omega\dot{Y} - 4\omega_o\overline{\Delta}z, \\ \ddot{Y} + (2\omega_o^2 - \Omega^2)Y &= -2\Omega\dot{X}, \\ \ddot{z} + 8(\omega_o^2 - \Delta^2)z &= -4\omega_o\overline{\Delta}(X - X_o). \end{aligned} \tag{26}$$

Here we denote by Δ the small frequency parameter

$$\Delta = \frac{\omega_o|B_o|}{\overline{B}} \ll \omega_o$$

and $\overline{\Delta} = (1 - B_o' X_o/2b)\Delta \approx \Delta$. The partial frequency of z oscillation, $\omega_z = \sqrt{8(\omega_o^2 - \Delta^2)}$, differs considerably from the natural frequencies $\Omega_\pm$ (given further by Eq. (27)) of coupled transverse oscillation. Because of that and since $\overline{\Delta}$ is small the coupling between the vertical and transverse oscillation is a tiny effect. We will neglect it for simplicity. On the contrary, the coupling between the X and Y oscillations is strong and should be taken into account carefully. The repulsing springs of partial X and Y oscillators of Eq. (26) are different and this is of importance resulting in a specific gyroscopic modulation of free oscillation, as elucidated below.

Evaluating from Eq. (26) the natural frequencies of transverse oscillation we obtain

$$\Omega_\pm^2 = \Omega^2 + \omega_+^2 \pm \sqrt{4\Omega^2\omega_+^2 + \omega_-^4} \tag{27}$$

where

$$\omega_\pm^2 = \omega_o^2 \pm \Delta^2.$$

The regime of small oscillation is stable unless $\Omega^2 < 2\omega_o^2$ (more about this condition is in Sec. VII). In view of $\Omega^2 \gg \omega_o^2$ the transverse oscillation reduces approximately to a simple form which after returning to the fixed coordinate frame is given by the complex function $\rho(t) = x(t) + iy(t)$

$$\rho(t) = X_o e^{i\Omega t} + (X_+ e^{i\omega t} + X_- e^{-i\omega t})e^{i\delta t}. \tag{28}$$

So $r_\perp(t) = |\rho(t)|$, $x(t) = \mathrm{Re}[\rho(t)]$ and $y(t) = \mathrm{Im}[\rho(t)]$. Here X_o is given by Eq. (24), $X_\pm$ are complex constants determined by initial conditions, Ω and $\Omega_\pm$ assumed (without loss of generality) positive, and

$$\begin{aligned} \omega &= \frac{\Omega_+ - \Omega_-}{2} \approx \omega_o \\ \delta &= \Omega - \frac{\Omega_+ + \Omega_-}{2} \approx \frac{\omega_o^4}{8\Omega^3}. \end{aligned} \tag{29}$$

As seen from Eq. (28) the normal transverse oscillations in the fixed coordinate frame are of different frequencies, $\omega + \delta$ and $\omega - \delta$, rather than of equal frequency [7]. The oscillations of different frequencies rotate in opposite directions. This results in the polarization of harmonic oscillation of frequency ω rotating slowly, at frequency δ, in the direction of the rotating magnetic field. This modulation which we call gyroscopic can be 100 % depending on the conditions of loading and manifests itself when the time of observation is commensurate or larger than $1/\delta$. The effect cannot be explained by the time-averaged potential concept and described in its terms. That concept results in a picture of degenerate transverse oscillation governed by averaged potential-like forces. It loses sight of gyroscopic forces induced by high frequency forces.

Another important feature we found is that the loading of atoms into the center $\boldsymbol{r} = 0$ and with zero velocity, does not eliminate the free oscillation and makes its amplitude larger than X_o by more than Ω/ω times:

$$\begin{aligned} \rho(t) &= \rho^{(o)}(t) \\ &= X_o\left\{e^{i\Omega t} - \left[i\frac{\Omega - \delta}{\omega}\sin(\omega t) + \cos(\omega t)\right]e^{i\delta t}\right\}. \end{aligned} \tag{30}$$

The physics is easy to understand noticing that the velocity oscillations $\dot{\rho}(t)$ of high and low frequency motion have nearly equal amplitudes.

For the case of nonzero initial conditions,

$$\rho(t) = \rho^{(o)}(t) + \rho^{(e)}(t)$$

with

$$\rho^{(e)}(t) = \left[\frac{\dot{\rho}(0) - i\rho(0)\delta}{\omega}\sin(\omega t) + \rho(0)\cos(\omega t)\right]e^{i\delta t} \tag{31}$$

where $\rho(0) = x(0) + iy(0)$ and $\dot{\rho}(0) = \dot{x}(0) + i\dot{y}(0)$. Provided $|\rho(0)|$ is of the same order or smaller than $|\dot{\rho}(0)|/\omega$, i.e. for loading close to the center of the trap, the two types of

motion, $\rho^{(o)}$ and $\rho^{(e)}$, become of same amplitude when the initial kinetic energy is about $M\Omega^2 X_o^2$. In terms of temperature $T_\perp$ of trapped atoms this corresponds to $T_\perp \approx T_\perp^{(o)}$ where

$$T_\perp^{(o)} = \frac{1}{k} M\Omega^2 X_o^2 = \frac{2\mu b}{k}\frac{\omega^2}{\Omega^2} \sim 1.4 \times 10^{-5}\ \mathrm{K}. \tag{32}$$

The numerical estimate is for the example $b = 10$ G, $\mu = \mu_B$ and $\omega/\Omega = 10^{-1}$. For the cited data, atomic mass $M = 40$ a.m.u. and static field gradient $B_o' = 10^2$ G/cm, we obtain roughly $B_o/b = 0.07$, $\omega/2\pi = 21$ Hz and $1/\delta = 0.6$ s. With this $X_o = 0.04$ mm and $|\rho^{(o)}(t)| \sim 0.4$ mm.

So, for the atoms loaded into the center of trap at a temperature $T_\perp$ small compared with $T_\perp^{(o)}$ the transverse size of the atomic spot is about $r_\perp = |\rho^{(o)}|$ which is independent of $T_\perp$ and given by the formulas and estimates above. In the opposite case, when $T_\perp \gg T_o$, approximately (for $|\dot\rho(0)| \gg \omega|\rho(0)|$)

$$\overline{r_\perp^2} = \frac{kT_\perp}{M\omega^2}. \tag{33}$$

The bar here and below means the average over the initial conditions and per period $2\pi/\omega$. The dependence on the motion of low frequency δ is retained but in the limit $|\dot\rho(0)| \gg \omega|\rho(0)|$ (and also when $|\dot\rho(0)| \ll \omega|\rho(0)|$) the gyroscopic modulation does not manifest itself in the mean square radius of the atom cloud. The radius is the same as for degenerate oscillation of frequency ω. As mentioned above the spring coefficient ω^2 can be made large compared to the transverse spring coefficient of an axial symmetry static trap and correspondingly the spot radius made much smaller. The vertical confinement of the top trap is even more strong, since $\omega_z^2 = 8\omega^2$. So, the atom spot in the case of an isotropic trapping temperature, $T_\perp = T_z$, is a flattened ellipsoid having a transverse diameter eight times larger than the vertical diameter.

The oscillation at which the trajectory touches the ring where the atoms leak from the trap due to spin-flips determines the bound on the atom spot size and, hence, the trapping temperature. As is obvious from Eq. (22) the points $\boldsymbol{r} = \boldsymbol{r}(t)$ where $B = 0$ are determined by

$$b = B_o' X/2, \quad Y = 0, \quad B_o + B_o' z = 0. \tag{34}$$

The distance z is small, $|z| = |B_o X/2b| \ll |X|$, and can be neglected. The trapping temperature given by Eq. (33) corresponding to a spot extending to the radius $r_\perp = 2|b/B_o'|$ equals

$$T_\perp = \frac{4M\omega^2 b^2}{kB_o'^2} = \frac{\mu b}{4k} \sim 1.7 \times 10^{-4}\ K. \tag{35}$$

The numerical estimate is for the same example as above. Only the rotating field magnitude enters the bound and the larger the field is, the larger the trapping temperature threshold. It is possible to arrange for fields several times larger than 10 G. But to increase the magnitude by orders of magnitude is difficult, since the rotating field coils should provide a uniform field of high frequency (~kHz).

Let us now consider polarization misalignment of atom spots which are small and do not extend near the ring where $B = 0$. The atomic polarization rotates around the z axis and a characteristic of interest is the spatial average of $\mu_x(\boldsymbol{r}, t)$. Say, a device is used which

critically depends on the polarization projection on axis x, rather than y or z. At the equilibrium orbit

$$\frac{\mu_x}{\mu} = -\frac{B_x(\boldsymbol{R}_o(t), t)}{B(\boldsymbol{R}_o)} = -\frac{b - B_o' X_o/2}{\overline{B}}\cos(\Omega t)$$

and the deviation of the averaged amplitude of rotation from the unperturbed rotation

$$\begin{aligned} P &= \frac{2}{\mu}\left|\overline{\cos(\Omega t)[\mu_x(\boldsymbol{r}(t), t) - \mu_x^{(o)}]}\right| \\ &\approx \left|\overline{\cos(\Omega t)\sum_{i,j=x,y,z} \tilde r_i(t)\tilde r_j(t)\frac{\partial^2}{\partial r_i \partial r_j}\frac{B_x}{B}}\right| \end{aligned} \tag{36}$$

[with $\mu_x^{(o)} = \mu_x(\boldsymbol{R}_o(t), t)$, $\tilde r_i = r_i - R_{oi}$ and the derivatives taken at $\boldsymbol{r} = \boldsymbol{R}_o(t)$] can be taken as a measure of misalignment. Evaluating this quantity in terms of trapping temperatures we obtain approximately

$$P = \frac{k}{4\mu b}\left\{T_z + T_\perp\left[\frac{1}{2} + \frac{\overline{(\dot x_o\cos(\delta t) - \dot y_o \sin(\delta t))^2}}{\overline{\dot x_o^2} + \overline{\dot y_o^2}}\right]\right\}. \tag{37}$$

At $\delta t \ll 1$ this equation reduces to

$$P = \frac{k}{4\mu b}(T_z + \frac{3}{2}T_x + \frac{1}{2}T_y).$$

T_x and T_y enter Eq. (37) unequally since the quantity B_x of Eq. (36) as a function of atom coordinate $\boldsymbol{r}$ depends on x and y differently. For isotropic initial conditions, when $\overline{\dot x_o \dot y_o} = 0$ and $T_z = T_\perp$, it follows from Eq. (37) that the upper temperature bound imposed by a given P is given by

$$T = \frac{4}{3}\frac{\mu b}{k}P \sim 0.5 \times 10^{-4}\ \mathrm{K}. \tag{38}$$

The numerical example is for $\mu = \mu_B$, $b = 10$ G and $P = 0.05$.

VII. TRAPPING BY SLOW ROTATING FIELDS

The top trap has a rather small spot size but not so good polarization alignment as seen from the bound (38). Besides, different "weak field seekers" appear in spots close to each other and to eliminate the atoms of unwanted ground states may cause problems. The area of atom leakage where the magnetic field periodically reduces to zero is rather close to the centre of the trap and this also limits the trapping abilities, as seen from the bound (35). Addressing these problems, we found that employing a rotating field of frequency Ω resonant to the orbital motion, rather than $\Omega \gg \omega_o$, represents a way to improve trapping characteristics.

The idea why the resonant orbit trap may have advantages comes from the analysis of equilibrium rotation of atoms. As seen from Eq. (24), when $\Omega^2 > 2\omega_o^2(X_o)$ the quantity $B_o' X_o$ is negative. Hence, the transverse field exerted by an atom trapped at the equilibrium orbit is larger than b:

$$\bar{b} = b - \frac{1}{2}B_o' X_o = \frac{\Omega^2 b}{\Omega^2 - 2\omega_o^2(X_o)} > b.$$

The smaller the resonance denominator is, the larger the effective rotating field $\bar{b}$. This quantity, rather than b, enters the important bounds.

The approach we developed in Sec. VI can be extended for the case of arbitrary Ω without difficulties. As Ω decreases the equilibrium radius X_o increases and the dependence $\omega_o^2(X_o)$ in Eq. (24) becomes significant. It makes the change of X_o and, hence, $\bar{b}$ finite for any Ω. Assuming as before $|B_o/\bar{b}| \ll 1$, we obtain approximately

$$X_o = -\frac{4b\omega_\phi^2}{B_o'\Omega^2}, \quad \frac{\bar{b}}{b} = 1 + \frac{2\omega_\phi^2}{\Omega^2} \tag{39}$$

and

$$\omega_o^2(X_o) = \frac{\Omega^2\omega_\phi^2}{\Omega^2 + 2\omega_\phi^2}, \quad \text{where} \quad \omega_\phi^2 = \frac{\mu B_o'^2}{8Mb}. \tag{40}$$

Noteworthy is that the resonance detuning

$$\Omega^2 - 2\omega_o^2(X_o) = \frac{\Omega^4}{\Omega^2 + 2\omega_\phi^2},$$

i.e. rapidly goes to zero as Ω decreases.

Besides Eq. (39), a different solution of Eq. (24) exists for all Ω. It results in positive $B_o'X_o$, $\bar{b}/b < 1$ and $2\omega_o^2(X_o) > \Omega^2$. But for an arbitrary ratio between Ω and ω_ϕ^2, this equilibrium solution is unstable with respect to small perturbations, while the solution given by Eq. (39) is stable. This follows from Eqs. (26) and (27) which are exact, provided the ω_o is understood to be a function of X_o, $\omega_o(X_o)$. The formulas of Sec. VI are modified beginning from Eq. (28).

Still, for Ω larger than or near ω_ϕ, the bounds as functions of Ω roughly follow the formulas of Sec. VI with ω_o and b substituted by $\omega_o(X_o)$ and $\bar{b}$ given by Eqs. (39) and (40). In particular, the trapping temperature bounds Eqs. (35) and (38), which relate $T_\perp$ to the spot size where leakage of atoms from the trap begins and to the level of polarization misalignment, take the form

$$T_\perp = \frac{\mu\bar{b}}{4k} \sim 3.3 \times 10^{-4}\ K\,,$$

$$T_\perp = \frac{4\mu\bar{b}P}{3k} \sim 10^{-4}\ K$$

where the numerical figures are for the example of Sec. VI and $\Omega^2 = 2\omega_\phi^2$. With this $X_o \sim 2$ mm.

So, the trapping temperatures can be significantly increased. As Ω decreases, the approximation of free oscillation in Eq. (28) by two frequency components, at $|\Omega - \Omega_-|$ and $|\Omega - \Omega_+|$, loses accuracy and the items of frequencies of $\Omega + \Omega_\pm$ neglected in Eq. (28) increase. The orbital motion $\mathbf{r}_\perp = \mathbf{r}_\perp^{(o)}(t)$ of the atoms loaded into the centre of the trap has five frequency components, $|\Omega \pm \Omega_\pm|$ and Ω. The scale of $r_\perp^{(o)}$ becomes of the same magnitude

as X_o. It is worth noting that by properly adjusting the loading one may change the orbit $\mathbf{r}_\perp^{(o)}(t)$ or reduce it to a circle of radius X_o. The dispersion of initial conditions results in the dispersion of $\mathbf{r}^{(\epsilon)}(t) = \mathbf{r}_\perp(t) - \mathbf{r}^{(o)}(t)$, rather than $\mathbf{r}^{(o)}(t)$, so we have the picture of an atom spot of mean size

$$\delta r_\perp = \sqrt{\overline{(r_\perp^{(\epsilon)}(t))^2}}$$

moving along the orbit $\mathbf{r}_\perp = \mathbf{r}_\perp^{(o)}(t)$.

Though the radius X_o increases by orders of magnitude compared to the top trap, the spot size $\delta r_\perp$ changes much less. Indeed, for a given dispersion of initial conditions this size behaves like $1/\omega_o(X_o)$. So the ratio $\delta r_\perp/X_o$ as a function of Ω and ω_ϕ behaves like $\Omega\sqrt{\Omega^2 + 2\omega_\phi^2}/\omega_\phi^3$ and rapidly goes to zero as Ω decreases. As a result, with the increase of X_o and $r_\perp^{(o)}$ there appears the possibility of separating clouds of trapped atoms having different ground states. The difference between equilibrium orbital radii for different values of μ/M increases like $1/\Omega^2$ and this allows one to arrange that the spots do not intersect.

One more advantage is that employing a rotating field frequency of a few tenths of a Hz, rather than a few kHz, makes it significantly easier to arrange large currents in the magnetic coils.

VIII. CONCLUSIONS

In the present work we developed a method of analysis based on a minimum of assumptions, and derived general relations and criteria concerning the trapping temperature for various types of magnetostatic traps, given small spot size and polarization misalignment parameters. We also discussed new ideas of trapping by rotating fields not previously elucidated in the literature.

It is widely believed that higher magnetic fields result in better trapping parameters. However, this is not totally correct as is evident from the presented results. Two classes of magnetic trap appear. For one class, including the axial and "coil + current bars" static field configurations, the trapping temperature does not depend on the field at all. In particular, for the axial symmetry traps the relation between the polarization misalignment, spot size and mean square velocity is a universal function containing no free parameters and is independent of the field and atomic mass and magnetic moment.

For the other class, including the baseball and Ioffe traps and the rotating field traps, the bounds on trapping temperatures strongly depend on the atomic magnetic moment and the magnetic field magnitude. Here the technical problems of arranging large fields limit the parameters.

The two bounds imposed on the trapping temperature, by restrictions on atom spot size and polarization misalignment, are different for all traps considered except the axial symmetry trap. The criterion for the latter (see Eq. (8)) is a function of the geometrical mean $\sqrt{\overline{r_\perp^2}P}$, while for the other types either $\overline{r_\perp^2}$ or P enter the temperature bound linearly. In the case of strong experimental requirements on the polarization misalignment the axial symmetry trap may have advantages, while for moderate P the baseball and Ioffe traps and rotating field traps provide better temperatures. The scales estimated in the text give a clear notion of what parameter values can be achieved in these cases.

We have paid much attention to the methods of trapping with rotating fields. For the top trap type the consideration has revealed important features of trapping lying beyond the time-averaged potential concept. A deep low-frequency gyroscopic modulation of atomic orbital motion takes place. Another specific feature is that the orbital motion of the atoms loaded in the trap center with zero velocity has a radius large compared with the radius of equilibrium orbit, X_o.

Finally, new methods of trapping with rotating magnetic field are proposed in the present work. They differ from the top type by employing the resonance between a low frequency rotating field and orbital motion, rather than a much higher rotating field frequency. At the expense of enlarging the radius of orbital motion, resonant orbit trapping allows one to increase the temperature bounds caused by polarization misalignment and leakage of atoms from the trap, facilitate the separation of particles of different ground states, and make arranging the rotating field of large amplitude easier.

ACKNOWLEDGMENTS

In the initial stage of this work O. Häusser provided me with relevant references. I would like to thank him and P. Jackson, A. Yavin, J. D'auria and J. Behr for their interest. Especially I am indebted to C.D.P. Levy for help with the English wording and to E. Vogt for arranging TRIUMF support and paying me much attention. Also essential for my work was C. Wieman's e-mail to O.H. informing him of the invention of the top trap by E.A. Cornell, and Cornell's comments to my preprint [8].

REFERENCES

[1] A.L. Migdal, J.V. Prodan, W.D. Phillips, T.H. Bergeman and H.J. Metcalf, Phys. Rev. Lett. **54**, 2596 (1985).

[2] V.S. Bagnato, G.P. Lafyatis, A.G. Martin, E.L. Raab, R.N. Ahmad-Bitar and D.E. Pritchard, Phys. Rev. Lett. **58**, 2194 (1987).

[3] H.F. Hess, G. Kochalski, J. Doyle, N. Masuhara, D. Kleppner and T. Greytak, Phys. Rev. Lett. **59**, 672 (1987).

[4] C.R. Monroe, W. Swann, H. Robinson and C.E. Wieman, Phys. Rev. Lett. **65**, 1571 (1990).

[5] C.E. Monroe, *Ph.D. Thesis*, (University of Colorado, Boulder, Colorado, 1992).

[6] H. Metcalf and P. van der Straten, Phys. Reports **244**, No 4-5, 203 (1994).

[7] W. Petrich, M.H. Anderson, J.R. Ensher and E.A. Cornell, A stable, tightly confining magnetic trap for evaporative cooling of neutral atoms. Draft: November 14, 1994, Physics Dept, University of Colorado, Boulder.

[8] V.E. Shapiro, Polarization criteria for magnetostatic traps for neutral atoms. Preprint, TRI-PP-94-83, Oct. 1994, TRIUMF, Vancouver, B.C.

FIGURES

FIG. 1. Two axial symmetry configurations. (a) The axial quadrupole. The currents of two coils are in opposite directions. The magnetic field vectors are shown by black arrows. (Figure from [6]). (b) The spherical hexapole. Three wires carry equal currents on the surface of a sphere.

FIG. 2. Three non-axial static field traps discussed in Secs. IV and V. (a) The "coil + current bar" trap. (b) The baseball trap. The external coil pair generating the magnetic field gradient which cancels gravity is not shown. (Figures (a) and (b) from Ref. [5]). (c) The Ioffe trap. Two coils form a "bottle field" and four vertical wires form a quadrupole field in the horizontal plane.

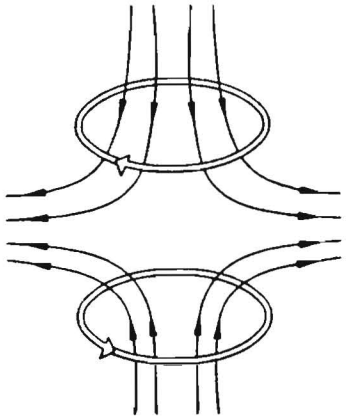

Fig. 1a

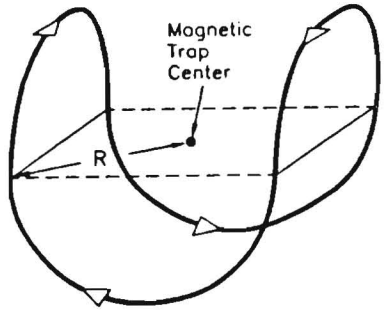

Fig. 2b

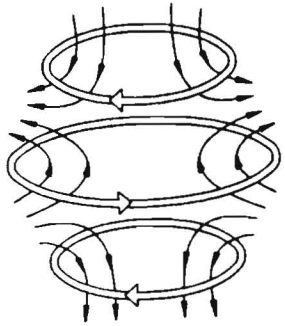

Fig. 1b

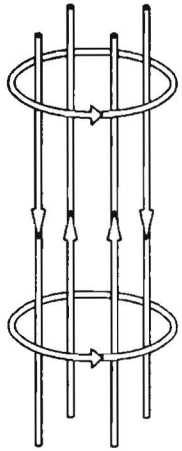

Fig. 2c

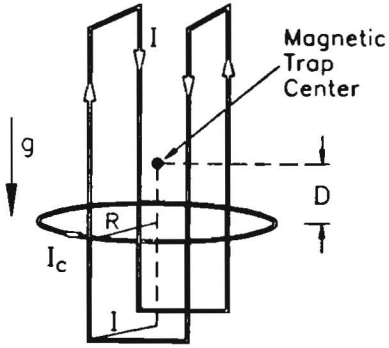

Fig. 2a